El Cezeri
Journal of Science and Engineering
ISSN: 2148-3736

Research Article

Optimization of Electro-Blown PVDF Nanofibrous Mats for Air Filter Applications

Ali Toptaş[1,2a], Mehmet Durmuş Çalışır[1,3b], Ali Kılıç[1,4c]
[1] TEMAG Labs, Faculty of Textile Tech and Design, Istanbul Technical University, Istanbul, Türkiye
[2] Safranbolu Vocational School, Karabuk University, Karabuk, Türkiye
[3] Faculty of Engineering and Architecture, Recep Tayyip Erdogan University, Rize, Türkiye
[4] Areka Group LLC, Istanbul, Türkiye

aalikilic@itu.edu.tr

DOI : 10.31202/ecjse.1391754
Received: 16.10.2023 Accepted: 12.02.2024
How to cite this article:
Ali Toptaş, Mehmet Durmuş Çalışır, Ali Kılıç, " Optimization of Electro-Blown PVDF Nanofibrous Mats for Air Filter Applications", El-Cezeri Journal of Science and Engineering, Vol: 11, Iss:2, (2024), pp.(199-206).
ORCID: [a]0000-0002-1176-0844; [b]0000-0002-5916-9666. [c]0000-0001-5915-8732;

Abstract : Particles with diameters smaller than 2.5 µm (PM2.5) have the capability to penetrate into respiratory system, thereby exerting adverse effects on human health. High-efficiency nanofiber mats present a viable and efficient solution for the purification of ambient air contaminated with such particulate matter. In this study, PVDF based electret nanofiber mats were optimized via electro-blowing technique. The experimental parameters were systematically devised utilizing a Taguchi three-level L9 orthogonal design, and the results were subsequently analyzed using ANOVA. In this context, among the examined parameters (solution concentration, air pressure, and electrical field), the most significant factors influencing fiber diameters were identified as solution concentration and electric field strength. While an increase in air pressure exhibited a negligible influence on fiber diameters, it was observed to mitigate undesired droplet density. The optimal parameters yielding the thinnest fiber (124 ± 71 nm) were determined as 9 wt.% solution concentration, 2 bar air pressure, and 30 kV electrical voltage. Furthermore, the application of corona discharge treatment to the specimens resulted in a remarkable enhancement of quality factors by over 70%.

Keywords : Nanofiber, Electro-Blowing Technique, Corona Discharge, Air filter

1 Introduction

In today's world, air pollution has reached critical levels due to the increasing number of fires, rapidly growing population, and industrial activities [1]. Air pollutants are classified based on their physical states as particulate matter and gaseous pollutants, while microorganisms like viruses and bacteria, metal ions, and fine/coarse particles constitute particulate matter and are further classified according to particle size [2]. Air filtration is an effective method to mitigate the problems arising from air pollution and provide clean and healthy air [3]. For this purpose, various types of air filters such as paper, membranes, woven or non-woven fabrics, etc., have been developed [4]. The primary goal in development efforts is to produce filters with high particle capture efficiency at an expense of low pressure drop (ΔP). Existing commercial high-efficiency particulate air filters (HEPA) have a filtration efficiency of at least 99.97% for aerosols and particles of $0.3\mu m$ and above [5, 6]. These filters are made from meltblown or glass fibers and there is a need for filters with fiber diameters in the range of 50nm to$1\mu m$ to effectively filter finer aerosols [6]. Filters with low pore size and high porosity layers can be produced using nanofibers with a high surface area-to-volume ratio [7]. However, this can lead to high ΔP in the filter media.

Electrospinning is one of the most common methods to produce nanofibers [8, 9, 10, 11, 12]. This method, where the driving force is an electrostatic field, enables the production of fine fibers with minimal defects (beads, droplets, etc.). However, it has the disadvantage of low solution feed rate and production rate [13]. Recently, the solution blowing method has been developed as an alternative, in which fibers are produced by the aerodynamic forces created by pressurized air acting on a polymer solution [14]. This system can achieve production speeds up to 20-50 times higher than electrospinning [15, 16, 17]. However, the solution blowing system suffers from irregularities in the produced fibers. The fibers tend to intertwine and form bundles due to the turbulence created by the pressurized air, leading to an increase in pore size [18]. The electro-blowing (EB) method combines the positive aspects of both electrospinning and solution blowing in a single configuration. In this method, there are two main forces acting on the polymer jet: electrical and air drag forces [19, 20, 21, 22, 23]. Compared to electrospinning, limited research has been conducted on nanofibrous air filter mats produced using the EB method [19, 20, 21].

Adding quasi-permanent electret properties to filter mats enhances filtration efficiency without increasing ΔP. Electret properties can be imparted to filters by using electret additives or electret fibers in the media, or by methods such as corona

discharge, triboelectrification, and liquid contact charging [24]. In this context, poly (vinylidene fluoride) (PVDF) polymer was investigated as an alternative material for the production of filter mats due to its thermal, chemical, and mechanical properties, as well as its effective electret properties [25]. Among all crystal phases of PVDF, only the β phase exhibits electret properties due to its net dipole moment [26]. The high electric forces used in electrospinning and electroblowing methods align the dipole moments of PVDF and promote crystallization in the β phase [19]. In a recent study, electrospun PVDF nanofiber membrane with an average fiber diameter (AFD) of 70 nm achieved which exhibited a high PM0.3 filtration efficiency of 97.40% with a low ΔP of 51 Pa at an air velocity of 5.3 cm/s [27]. Another study investigated the performance of electrospun PVDF nanofibers with different diameters (84–525 nm) against various aerosols after applying corona discharge. Filter efficiency against 100 nm NaCl aerosols increased from 30% to 61.9% with corona charging for filters composed of 84 nm fibers [28]. Electrospun PVDF nanofiber mat with ultra-thin nanonet structures achieved a filtration efficiency of 99.999% and a ΔP of 124.2 Pa [5].

In engineering and scientific fields, experimental design and parameter optimization are of critical importance for the effective analysis and improvement of processes and systems. In this regard, statistical techniques such as "Design of Experiments" (DOE) and the "Taguchi Method" play a significant role [29]. The Taguchi Method enables the acquisition of information about the entire parameter space with a small experimental unit through a specially designed orthogonal pattern. The advantage of the method lies in its ability to analyze multiple components simultaneously and consider uncontrollable noise factors [30].

Upon examining research aimed at optimizing nanofibers through the Taguchi method, it becomes apparent that investigations have been carried out with electrospinning method on a variety of polymers, including poly(acrylamide), poly (acrylic acid), and poly (vinyl alcohol) [31], PVP [32], PVDF [33, 34]. Conversely, Akgul et. al. [35] employed the centrifugal spinning method along with Taguchi to find the optimum parameters in the production of thermoplastic polyurethane nanofibers for air filter applications. A literature search on studies related to electro-blowing and Taguchi reveals only that Saraç [36] utilized the Taguchi method to determine the process parameters for the thinnest polysulfone (PSU) nanofibers with the minimum defects, reporting the optimal conditions as 13 wt% PSU, 3 bar, and 7.5 kV. Notably, no study incorporating the combination of PVDF with electro-blowing and Taguchi has been identified in the literature.

In this study, the material and process parameters of electro-blown PVDF nanofiber filter mats were optimized using the Taguchi experimental design approach. The system parameters (electric field and air pressure), and the material parameter (solution concentration), were considered and three levels (low, moderate, high) were defined for each of parameters. Additionally, samples obtained under the optimum condition were reproduced without applying an electric field to investigate the influence of the electric field on fiber diameter and filtration characteristics. Changes in filtration performance of samples treated with corona discharge were also compared.

2 Experimental Methods

2.1 Materials

Polyvinylidene fluoride (PVDF) with a molecular weight of 477,000 g/mol (Kynar Flex 2801-00) was purchased from Arkema (France). Dimethyl sulfoxide (DMSO) of 99.8% purity (Merck), and acetone of 99.5% purity from ISOLab, were chosen as the solvents. The solutions were prepared by adding the PVDF powders into DMSO and acetone mixture (70/30 wt/wt) to obtain final polymer concentrations of 9%, 12%, and 15% by weight and mixing at a temperature of 70°C using a magnetic stirrer for a duration of 8 hours.

2.2 Nanofiber Production

Fiber production was carried out using the electro-blowing system AeroSpinner L1.0 (Areka Group Ltd.) that is schematically shown in Figure 1. Parameters used during fiber production in the EB system can be grouped into material (solution concentration, solution type, viscosity, etc.), process (air pressure, electrical field, feeding rate, collector distance, etc.), and environmental parameters (humidity, temperature).

In the experimental design, the three most important parameters (concentration, air pressure, and electrical voltage) were used as Taguchi design factors, and a three-level L9 orthogonal design was created as shown in Table 1.

Table 1: Design of experiment produced with Taguchi

Sample IDs	Solution concentration (%)	Air Pressure (bar)	Electric Voltage (kV)	AFD (nm)
1	9	1	10	209.5 $\pm$ 46.3
2	9	2	20	172.4 $\pm$ 46.2
3	9	3	30	154.7 $\pm$ 54.6
4	12	1	20	259.1 $\pm$ 63.1
5	12	2	30	217.6 $\pm$ 72.0
6	12	3	10	266.5 $\pm$ 107.2
7	15	1	30	324.3 $\pm$ 86.5
8	15	2	10	381.5 $\pm$ 74.0
9	15	3	20	368.5 $\pm$118.2

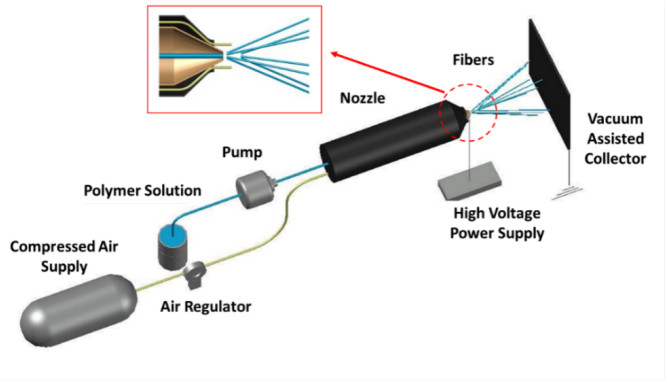

Figure 1: Schematic presentation of the electro-blowing setup

For all experiments, feeding rate, collector distance, collector rotation speed and production time were kept constant as 10 mL/h, 30 cm, 40 rpm, and 20 minutes, respectively. The produced fibers were collected onto spunbond fabrics with an average fiber diameter (AFD) of $14 \pm 2.1\ \mu m$.

2.3 Characterization

The viscosities of the PVDF solutions were measured using a rotational viscometer (Fungilab, α Series) immediately before fiber production, and they were determined as 356.5, 487.3, and 654.2 mPa·S for solution concentrations of 9, 12, and 15 wt.%, respectively. The morphological analyses of the produced fibers were conducted using a TESCAN VEGA3 Scanning Electron Microscope (SEM). SEM images were taken at 5kx magnification, and the average fiber diameters and distributions, along with standard deviation values, were calculated using 100 measurements for each sample on the Image J program.

Signal-to-noise (S/N) ratios and Analysis of Variance (ANOVA) were performed for each level of the parameter to determine the optimum parameter levels using Minitab 18 Software. In the Taguchi method, the S/N ratio can be defined with three approaches: Smaller-the-better, larger-the-better, and nominal-the-best [37]. In this study, the S/N ratio is calculated using the smaller-the-better approach with Eq 1 [38]. Here, y_i represents the value of the average fiber diameter of the ith experiment at the lower level of each factor, and n is the number of experiments conducted for this factor and level. Air permeability related to the thickness and porosity of the fibrous mat is an important factor used to determine filter performance.

$$\frac{s}{N} = -10 \log \left(\frac{1}{n} \sum_{i=1}^{n} y_i^2 \right) \tag{1}$$

Air permeability testing device (Airtest II, Prowhite) was employed in accordance with ASTM D737 standards. The test conditions encompassed a sample diameter of 38 cm^2, air pressure of 125 Pa, and an ambient temperature maintained at 22 ± 2 °C. The ΔP and filtration efficiency values of the produced samples were determined using an automated filter tester (8130A, TSI Inc.). Sodium chloride (NaCl) aerosols in the range of $0.26 \pm 0.07\ \mu m$ were generated from a NaCl solution with a wt. concentration of 2%. Filter samples with an effective area of 100 cm^2 were tested against aerosols produced at a face velocity of 15.83 cm/s. Corona charging was performed using a negative corona discharger (Chargemaster 5, Simco Ion). For corona application, the device's electrode was positioned approximately 4 cm above a rotating drum. Nanofiber samples were placed on the drum and charged for 5 minutes under a charging voltage of -20 kV while rotating at 23 rpm.

3 Results and Discussion

3.1 Fiber Morphology

The SEM images of the samples are presented in Figure 2. Accordingly, the impacts of solution concentration on both fiber production and morphology are evident. Irrespective of the other parameters, augmenting the solution concentration exhibited a favorable influence on fiber formation across all samples. The quantity of droplets within the samples (samples 1-6) diminished as the solution concentration increased, and no droplets were discernible within samples derived from a 15 wt.% solution. In addition, the increase in both the air pressure and the electric field in for the production from 9-wt. % solution also decreased the density of droplets on the mat. While the mean fiber diameters for all specimens were sub-micron, the augmentation of solution concentration yielded thicker fibers.

Samples produced using a 9 wt.% solution (1-3) manifested the thinnest fibers. The increase of air pressure and electric field induced an additional reduction in fiber diameter. The synergy of these two driving forces caused the low-viscosity solution jet to attenuate, enabling the production of fibers with diameters below 250 nm. Elevating the solution concentration from 9% to 12% yielded an increment in fiber diameter. On the other hand, the simultaneous increase of air pressure and electric field

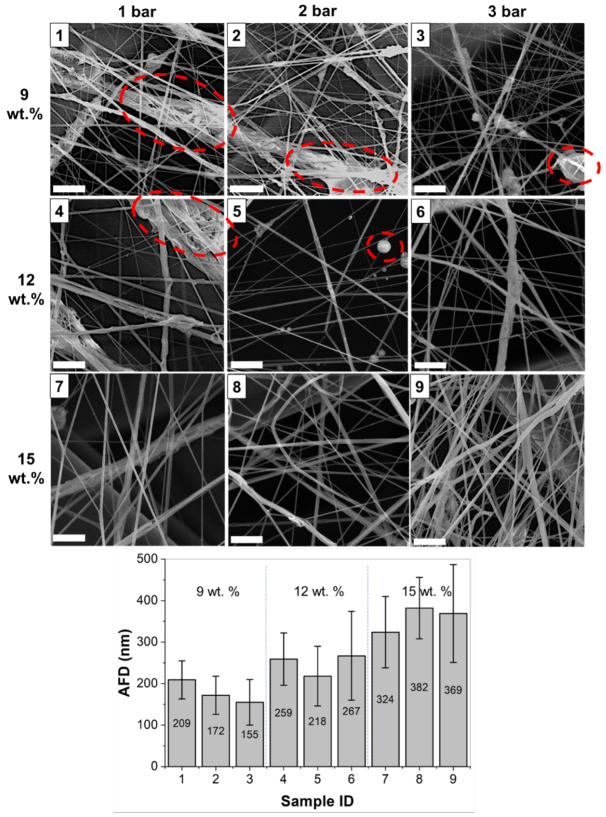

Figure 2: SEM images of the samples produced according to the Table 1 (scale bars are 5 μm) and their AFDs

decreased the mean fiber diameter from 257 nm (sample 4) to 220 nm (sample 5). In sample 6, despite application of the highest air pressure (3 bar), diminishing the electric field to 10 kV led to reduction of fiber diameter to 265 nm. Among the samples produced from the 12 wt.% solution, sample 6 produced with the lowest electric field showed the highest fiber diameter. This underscores the preeminence of the electric field in influencing fiber diameter compared to air pressure.

The coarsest fibers were derived from a 15 wt.% solution. Analogously, the increasing of air pressure coupled with the reduction of the electric field yielded thicker fibers for samples 7 and 8. This reaffirms the preeminence of the electric field over air pressure in terms of influencing fiber diameter. Conversely, in samples 8 and 9, the simultaneous escalation of both propulsive forces led to a diminution in fiber diameter.

In conclusion, lower solution concentration correlates with a reduction in average fiber diameters and a concurrent increment in droplet density. In other words, higher solution concentration results in lower droplet density, accompanied by an increment in fiber diameters. Moreover, the influence of the electric field on fiber diameters is less pronounced than that of solution concentration, yet more pronounced than air pressure.

3.2 Determination of Optimum Conditions

As the signal increases, variance is expected to decrease, making the maximization of the Signal-to-Noise (S/N) ratio the goal of the study for determining optimal parameters. The S/N ratios calculated based on the mean fiber diameters of the design factors are presented in Table 2. Here, "Level 1" corresponds to the S/N ratios of the first level of each design factor, while "Level 2" and "Level 3" correspond to the second and third levels, respectively. Additionally, delta represents the maximum difference among the S/N ratios calculated for each factor at the three levels, whereas rank signifies the efficacy value of the factors for obtaining the lowest fiber diameter. Accordingly, rank is 1 for the highest delta value, and 3 for the lowest delta value. The factor with rank 1 exerts the most significant influence on fiber diameters. In Table 2, the solution concentration of 9 wt.% yielding the maximum S/N ratios, along with 2 bar air pressure and 30 kV electric field, is recommended as the optimal condition for achieving the thinnest fiber. These conditions represent the optimal configuration for achieving the lowest fiber diameter among all possible conditions (27 experiments). This scenario can be further elucidated through analysis of variance (ANOVA).

ANOVA is utilized to examine and assess statistical differences among distinct groups, probing the determination of whether the variance between these groups arises haphazardly or possesses statistical significance. Initially, through computation of the collective between-group and within-group variances, the adjusted sum of squares (Adjusted SS) is ascertained between the groups. This Adjusted SS is divided by the degrees of freedom to yield the Adjusted MS. The F-value conveys the proportion

Table 2: S/N ratios of the design factors for "Smaller is better"

	Solution concentration (%)	Air Pressure (bar)	Electric Voltage (kV)
Level 1	-44.99	-48.26	-48.86
Level 2	-47.84	-47.72	-48.08
Level 3	-51.06	-47.90	-46.95
Delta	6.07	0.53	1.91
Rank	1	3	2

of between-group variance relative to within-group variance. Consequently, the detection of substantial differences between groups signifies the origination of these differences stem from expected causes. A high F-value indicates a significant difference between groups, while a low F-value implies the insignificance of differences between groups. On the other hand, the p-value serves to determine the import of statistical test outcomes and embodies the probability correspondent to the derived F-value. This value is employed to determine whether the observed difference is statistically significant or occurred by chance and a p-value typically less than 0.05 is considered statistically significant.

As per the ANOVA outcomes outlined in Table 3, the levels applied to polymer solution concentration exhibit statistical significance, substantiated by a p-value of 0.008. Since the largest contribution to the total Adj SS ratio (90.1%) comes from solution concentration, the concentration has been identified as the most effective parameter using the "smaller is better" approach for the average fiber diameter. On the other hand, the p-value of the electric field can be interpreted as statistically significant with a value of 0.08, while the p-value for air pressure is far from statistical significance at 0.867. Similarly, the contribution of the electric field in the total Adj SS ratio is 8.2%, while the contribution of air pressure is 0.001%. Furthermore, due to interactions among factors, the ANOVA results exhibit an error rate of 0.007%.

Considering these findings, increasing air pressure did not manifest a noteworthy impact on fiber diameter for electro-blown fibrous mats from PVDF/DMSO-Acetone solution while it caused the reduction of the droplet density. However, it is noteworthy that Yusuf et al. [39], in their experimental and modeling-based study utilizing the solution-blowing methodology, disclosed that elevating air pressure from 1 bar to 3 bar engenders a reduction in fiber diameters while further escalation from 3 bar to 6 bar resulted in thicker fiber in diameter. This underscores there is a critical threshold for air pressure within the solution-blowing method to achieve thinner fiber. Over this critical value fibers get stacked to form a bundled structure because of air turbulence. As per our study, in the EB approach, the presence of an electric field near the air drag forces implies producing additional force to attenuate the polymer jet, therefore there is no observed critical threshold for reducing fiber diameter between 1 - 3 bar. This critical threshold may occur at lower air pressures, thus, an exploration of lower air pressure levels (0.5, 1, 1.5 bar) is advisable.

Table 3: Analysis of Variance for means

Source	DF	Adj SS	Adj MS	F-Value	P-Value
Solution concentration	2	49150.9	24575.4	127.04	0.008
Air Pressure	2	59.6	29.8	0.15	0.867
Electric Voltage	2	4422.9	2211.4	11.03	0.080
Error	2	386.9	193.4		
Total	8	54020.2			

3.3 Confirmation Test

The estimated average fiber diameter $(\mathrm{AFD_{est}})$ of the fibers to be produced under the specified optimal conditions of 9 wt.% concentration, 2 bar air pressure, and 30 kV electric voltage can be calculated using the following formula (Equation 2).

$$AFD_{est} = \bar{X} + (\bar{C}1 - \bar{X}) + (\bar{P}2 - \bar{X}) + (\bar{V}3 - \bar{X}) \tag{2}$$

Here, $\overline{X}$ represents the AFD of 9 samples produced according to the Taguchi design. $(\bar{C}1)$ corresponds to the AFD of all samples produced from 9 wt.% solution (samples 1 – 3), similarly $(\bar{P}2)$ represents the AFD of samples produced with 2 bar air pressure (samples 2, 5, 8), and $(\bar{V}3)$ represents the AFD of samples produced with 30 kV electrical voltage (samples 3, 5, 7). Accordingly, the $(\mathrm{AFD_{est}})$ is calculated as 143 nm. Under these optimal conditions, sample 10 was produced and its SEM image and AFD graphs are provided in Figure 3. This sample has the smallest fiber diameter among all samples produced, with a size of 124 $\pm$ 71 nm. To observe the effect of the electric field on this sample, sample 11 was produced without an electric field. According to the SEM image in Figure 3, the absence of an electric field has increased the fiber diameter (206 $\pm$ 148 nm) and increased the droplet size in the structure (> 5 μm).

3.4 Filtration Performance

The filtration efficiency and ΔP values before and after corona treatment for all samples are presented in Figure 4. The highest filtration efficiency (91.87%) was achieved from sample 10, which was produced at the optimum parameters obtained from the ANOVA analysis and had the thinnest fiber diameter. On the other hand, the lowest filtration value (80.55%) was obtained from sample 8, which had the thickest fibers with an AFD value of 382 nm. According to the ANOVA results, solution concentration is

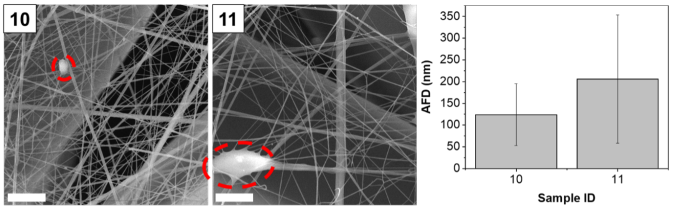

Figure 3: SEM images (scale bars are 5 μm) and AFD of samples 10 and 11

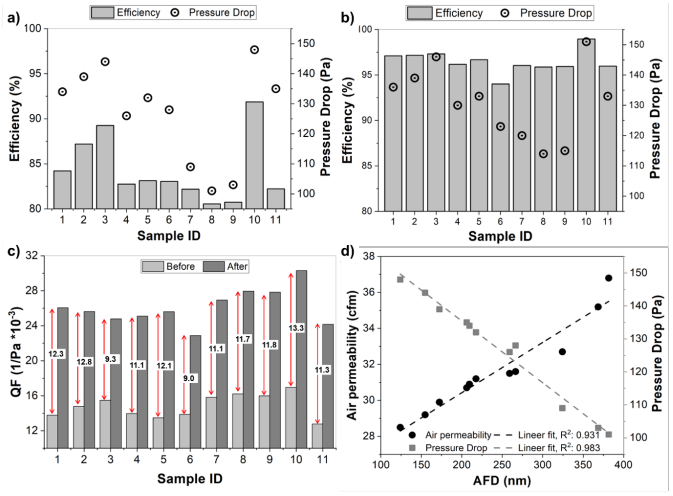

Figure 4: Filtration efficiency and ΔP of the samples a) before, b) after corona treatment. c) QF values, and d) air permeability and ΔP of the samples against AFDs

the most influential parameter on fiber diameters. This observation is similarly reflected in the filtration results. Lower solution concentration values result in finer fibers and consequently higher filtration efficiency (samples 1-3), while higher solution concentration solutions lead to thicker fibers and lower filtration efficiency (samples 7-9).

A similar trend is observed in the ΔP values, as shown in Fig. 4a. The highest and lowest ΔP values of 148 Pa and 101 Pa were obtained from the fine fibrous mat (sample 10) and thickest fibrous mat (sample 8), respectively. This is attributed to the restricted airflow due to the small pores created by fine nanofibers. When comparing samples 1 and 11, which have a similar fiber diameter, it is noted that the ΔP are nearly the same (134 and 135 Pa), but sample 1 exhibits better filtration performance because of the applied electrical voltage. This difference in filtration efficiency highlights the contribution of the electret effect demonstrated by PVDF nanofibers produced in the presence of an electrical field to the filtration mechanism. An enhancement in filtration efficiency was observed in all samples with the Corona Discharge treatment (Figure 4b). The increase in filtration efficiency is consistent with the initial performance of the samples. The highest filtration efficiency of 98.97% was achieved in the optimum sample (sample 10). After corona treatment, the lowest filtration performance increased to a value of 94.01% from 80.55%.

The quality factor (QF) values, which represent one of the most crucial parameters determining filter performance, are presented in Fig. 4c. Before corona treatment, the highest QF value (0.0170) was observed from sample 10. An inverse relationship between fiber diameter and QF values is evident. Corona treatment has notably enhanced the QF values across all samples. The most substantial enhancement, with a significant increase of 78.7%, was achieved in sample 10. This can be attributed to the heightened efficacy of the Corona Discharge treatment on sample 10 because of the finer fibrous structure that provided a higher surface area. The air permeability test results for the samples are depicted in Fig. 4d, in accordance with the AFD values. It is evidently observed that a linear relationship exists between fiber diameters and air permeability, whereby an increase in AFD corresponds to elevated air permeability values. This correlation is further reflected in the ΔP results and found similar with the other reported studies [40]. The sample with the highest air permeability also exhibited the lowest ΔP value. The calculated determination coefficients of the linear fit at 0.93 and above, signify the reliability of the explanation above.

4 Conclusion

In this study, PVDF nanofiber air filter production was optimized using novel electro-blowing technique. Based on the three-level L9 orthogonal Taguchi design, the effects of solution concentration, air pressure, and electric field on fiber diameter were systematically investigated. The significance of these parameters was also analyzed with ANOVA. According to the results,

solution concentration and applied electrical field value were found as the main factors affecting the fiber diameters. Although air pressure variations have a limited impact on diameters, they influenced droplet density, resulting in higher air pressure leading to lower droplet density. The optimum levels for the finest fiber diameter were found as 9% by weight solution concentration, 2 bar air pressure, and 30 kV electrical voltage. In addition, the corona discharge process increased the filtration performance to 98.97% in the best sample, resulting in a 78.7% improvement in the QF. This study highlights the potential of the electro-blowing method in the processing of high-efficiency PVDF nanofibers for air filtration.

Acknowledgements

This work was supported by Scientific Research Projects Coordination Unit of Istanbul Technical University (ITU BAP Grant Number MGA-2023-44749). The authors gratefully acknowledge AREKA Advanced Technology Ltd. Comp., (www.arekananofiber.com) for the electro-blowing system.

Authors' Contributions

AT conducted the experiments and fabricated the samples. All authors performed the theoretical calculations, contributed to the writing of the article, and reviewed and approved the final manuscript.

Competing Interests

The authors declare that they have no competing interests.

References

[1] A. Valavanidis, K. Fiotakis, and T. Vlachogianni. Airborne particulate matter and human health: Toxicological assessment and importance of size and composition of particles for oxidative damage and carcinogenic mechanisms. *Journal of Environmental Science and Health, Part C*, 26(4):339–362, 2008.

[2] M. He, T. Ichinose, M. Kobayashi, K. Arashidani, S. Yoshida, M. Nishikawa, H. Takano, G. Sun, and T. Shibamoto. Differences in allergic inflammatory responses between urban pm2.5 and fine particle derived from desert-dust in murine lungs. *Toxicology and Applied Pharmacology*, 297:41–55, 2016.

[3] R. Zhang, C. Liu, P. Hsu, C. Zhang, N. Liu, J. Zhang, H. R. Lee, Y. Lu, Y. Qiu, S. Chu, and Y. Cui. Nanofiber air filters with high-temperature stability for efficient pm2.5 removal from the pollution sources. *Nano Letters*, 16(6):3642–3649, 2016.

[4] J. Liu, D. Y. H. Pui, and J. Wang. Removal of airborne nanoparticles by membrane coated filters. *Science of The Total Environment*, 409(22):4868–4874, 2011.

[5] Z. Li, W. Kang, H. Zhao, M. Hu, J. Ju, N. Deng, and B. Cheng. Fabrication of polyvinylidene fluoride tree-like nanofiber web for ultra high performance air filtration. *Material Design*, 92:95–101, 2016.

[6] J. L. Davis, H. J. Walls, L. Han, T. A. Walker, J. A. Tufts, A. Andrady, and D. Ensor. Use of nanofibers in high-efficiency solid-state lighting. In *Seventh International Conference on Solid State Lighting*, pages 248–256. SPIE, 2007.

[7] A. Kilic, S. Selcuk, A. Toptas, and A. Seyhan. *Nonelectro nanofiber spinning techniques*, chapter 10, pages 267–293. Elsevier, 2023.

[8] M. Aliabadi. Effect of electrospinning parameters on the air filtration performance using electrospun polyamide-6 nanofibers. *Chemical Industry and Chemical Engineering Quarterly*, 23(4):441–446, 2017.

[9] P.-Y. Chen and S.-H. Tung. One-step electrospinning to produce nonsolvent-induced macroporous fibers with ultrahigh oil adsorption capability. *Macromolecules*, 50(6):2528–2534, 2017.

[10] X. Ding, Y. Li, Y. Si, X. Yin, J. Yu, and B. Ding. Electrospun polyvinylidene fluoride/sio2 nanofibrous membranes with enhanced electret property for efficient air filtration. *Composites Communications*, 13:57–62, 2019.

[11] T. Tanski, P. Jarka, and W. Matysiak. *Electrospinning Method Used to Create Functional Nanocomposites Films*. InTech, 2018. . URL `http://dx.doi.org/10.5772/intechopen.70984`.

[12] M. Ekrem. Mechanical properties of mwcnt reinforced polyvinyl alcohol nanofiber mats by electrospinnig method. *El-Cezeri*, 4(2), 2017.

[13] M. Xia, Q. Liu, Z. Zhou, Y. Tao, M. F. Li, K. Liu, Z. Wu, and D. Wang. A novel hierarchically structured and highly hydrophilic poly(vinyl alcohol-co-ethylene)/poly(ethylene terephthalate) nanoporous membrane for lithium-ion battery separator. *Journal of Power Sources*, 266:29–35, 2014.

[14] Y. Polat, E. S. Pampal, E. Stojanovska, R. Simsek, A. Hassanin, A. Kilic, A. Demir, and S. Yilmaz. Solution blowing of thermoplastic polyurethane nanofibers: A facile method to produce flexible porous materials. *Journal of Applied Polymer Science*, 133(9), 2016.

[15] H. Lou, W. Han, and X. Wang. Numerical study on the solution blowing annular jet and its correlation with fiber morphology. *Industrial & Engineering Chemistry Research*, 53(7):2830–2838, 2014.

[16] M. Gungor, S. Selcuk, A. Toptas, and A. Kilic. Aerosol filtration performance of solution blown pa6 webs with bimodal fiber distribution. *ACS Omega*, 7(50):46602–46612, 2022.
[17] M. Gungor, M. D. Calişir, and A. Kilic. Solution-blown pa6- and pvdf-based nanofibrous composite mats for aerosol filtration. *Fibers and Polymers*, 24(5):1603–1612, 2023.
[18] L. Shi, X. Zhuang, X. Tao, B. Cheng, and W. Kang. Solution blowing nylon 6 nanofiber mats for air filtration. *Fibers and Polymers*, 14(9):1485–1490, 2013.
[19] A. Al Rai, E. Stojanovska, G. Fidan, E. Yetgin, Y. Polat, A. Kilic, A. Demir, and S. Yilmaz. Structure and performance of electroblown pvdf-based nanofibrous electret filters. *Polymer Engineering and Science*, 60(6):1186–1193, 2020.
[20] A. Eticha, A. Toptaş, Y. Akgül, and A. Kilic. Electrically assisted solution blow spinning of pvdf/tpu nanofibrous mats for air filtration applications. *Turkish Journal of Chemistry*, 47(1):47–53, 2023.
[21] M. Gungor, A. Toptas, M. D. Calisir, and A. Kilic. Aerosol filtration performance of nanofibrous mats produced via electrically assisted industrial-scale solution blowing. *Polymer Engineering and Science*, 61(10):2557–2566, 2021.
[22] L. Cao, Q. Liu, J. Ren, W. Chen, Y. Pei, D. L. Kaplan, and S. Ling. Electro-blown spun silk/graphene nanoionotronic skin for multifunctional fire protection and alarm. *Advanced Materials*, 33(38):2102500, 2021.
[23] Y. Liu, C. Jia, H. Zhang, H. Wang, P. Li, L. Jia, F. Wang, P. Zhu, H. Wang, L. Yu, F. Wang, L. Wang, X. Zhang, Y. Sun, and B. Li. Free-standing ultrafine nanofiber papers with high pm0.3 mechanical filtration efficiency by scalable blow and electro-blow spinning. *ACS Applied Materials and Interfaces*, 13(29):34773–34781, 2021.
[24] A. Kilic, S. Russell, E. Shim, and B. Pourdeyhimi. *The charging and stability of electret filters*, chapter 4, pages 95–121. Woodhead Publishing Series in Textiles. Woodhead Publishing, 2017.
[25] D. Lolla, M. Lolla, A. Abutaleb, H. U. Shin, D. H. Reneker, and G. G. Chase. Fabrication, polarization of electrospun polyvinylidene fluoride electret fibers and effect on capturing nanoscale solid aerosols. *Materials*, 9(8), 2016.
[26] A. J. Lovinger. Ferroelectric polymers. *Science*, 220(4602):1115–1121, 1983.
[27] T. T. Bui, M. K. Shin, S. Y. Jee, D. X. Long, J. Hong, and M. G. Kim. Ferroelectric pvdf nanofiber membrane for high-efficiency pm0.3 air filtration with low air flow resistance. *Colloids and Surfaces A: Physicochemical and Engineering Aspects*, 640:128418, 2022.
[28] W. W. F. Leung and Q. Sun. Electrostatic charged nanofiber filter for filtering airborne novel coronavirus (covid-19) and nano-aerosols. *Separation and Purification Technology*, 250:116886, 2020.
[29] H. M. Khanlou, B. C. Ang, S. Talebian, A. M. Afifi, and A. Andriyana. Electrospinning of polymethyl methacrylate nanofibers: optimization of processing parameters using the taguchi design of experiments. *Textile Research Journal*, 85 (4):356–368, 2015.
[30] J. Stufken and G. S. Peace. Taguchi methods: A hands-on approach. *Technometrics*, 36(1):121, 1994.
[31] T. S. Sorkhabi, M. F. Samberan, K. A. Ostrowski, P. Zajdel, A. Stempkowska, and T. Gawenda. Electrospinning of poly (acrylamide), poly (acrylic acid) and poly (vinyl alcohol) nanofibers: Characterization and optimization study on the effect of different parameters on mean diameter using taguchi design of experiment method. *Materials*, 15(17), 2022.
[32] A. Pinarbasi and F. C. Callioglu. Electrospinning of pvp nanofibers and optimization with taguchi experimental design. *Süleyman Demirel University Faculty of Arts and Science Journal of Science*, 17(2), 2022.
[33] A. Tariq, A. H. Behravesh, Utkarsh, and G. Rizvi. Statistical modeling and optimization of electrospinning for improved morphology and enhanced β-phase in polyvinylidene fluoride nanofibers. *Polymers*, 15(22), 2023.
[34] S. Gee, B. Johnson, and A. L. Smith. Optimizing electrospinning parameters for piezoelectric pvdf nanofiber membranes. *Journal of Membrane Science*, 563:804–812, 2018.
[35] N. A. S. Gundogdu, Y. Akgul, and A. Kilic. Optimization of centrifugally spun thermoplastic polyurethane nanofibers for air filtration applications. *Aerosol Science and Technology*, 52(5):515–523, 2018.
[36] Z. Sarac, A. Kilic, and C. Tasdelen-Yucedag. Optimization of electro-blown polysulfone nanofiber mats for air filtration applications. *Polymer Engineering and Science*, 63(3):723–737, 2023.
[37] H. Oktem, T. Erzurumlu, and I. Uzman. Application of taguchi optimization technique in determining plastic injection molding process parameters for a thin-shell part. *Materials and Design*, 28(4):1271–1278, 2007.
[38] H.-L. Lin and C.-P. Chou. Optimization of the gta welding process using combination of the taguchi method and a neural-genetic approach. *Materials and Manufacturing Processes*, 25(7):631–636, 2010.
[39] Y. Polat, M. Yangaz, M. D. Calisir, M. Z. Gül, A. Demir, B. Ekici, and A. Kilic. Çözeltiden üfleme ile nanolif üretim yönteminde hava basıncının nanolif üretimine etkisi. *Journal of the Faculty of Engineering and Architecture of Gazi University*, 35(4), 2020.
[40] A. Toptaş, M. D. Çalışır, and A. Kılıç. Production of ultrafine pvdf nanofiber-/nanonet-based air filters via the electroblowing technique by employing peg as a pore-forming agent. *ACS Omega*, 2023.